

Common Computational Principles Underlying Texture Processing in Vision and Touch

A Introduction

Goal: The goal of this project is to identify and validate common computational principles underlying visual and tactile texture processing in the brain.

Background: The sensory cortices are fairly uniform in their anatomical layout, however, at the same time they are highly specialized for specific sensory modalities [90, 104]. It is also known that they are highly plastic: Rewiring can cause the sensory cortex to serve different modalities other than its native modality (e.g., visual response observed in rewired auditory cortex: [105]). This points to common computational principles underlying information processing across different sensory modalities.

Motivation: In order to identify common computational principles, it is necessary to start from a specific aspect of sensory processing that is common across all modalities under consideration. It turns out that texture is a significant feature in vision [49, 116, 117], touch [44, 97], and even in audition [80]. Thus, texture can serve as a unifying stimulus feature that can be used to probe for common computational principles shared by different sensory modalities.

Approach: In this project, we will employ anatomical, physiological, behavioral, and computational approaches to identify and validate common computational principles underlying texture processing in the mouse cortex, focusing on vision (visual cortex: [88]; see [5] for a general discussion on the feasibility of vision research in the mouse) and touch (somatosensory cortex: [25, 44]).

Objectives: The objectives of this project are as follows. (1) Behavioral characterization of visual vs. tactile texture processing in the mouse. (2) Electrophysiological measures of visual vs. tactile texture processing in the mouse. (3) Anatomically-correct, large-scale circuit simulation with multicompartmental neuron models of the visual and the somatosensory cortex of the mouse. (4) Computational modeling of visual vs. tactile texture processing. (5) Analysis of the above data to derive common computational principles underlying texture processing in the sensory cortex. (6) Predictions from the computational principles and experimental validation.

Intellectual merit: The sensory cortices are both general and specific in terms of their structure and function. By investigating an abstract stimulus feature that is common to two or more sensory modalities (e.g. texture), it will be possible to extract common computational principles underlying sensory cortical processing. The multi-pronged approach ranging from behavioral, physiological, anatomical, to computational, will result in high quality, correlated data, each valuable on its own, and more so when considered together.

Broader impacts: As part of the project, graduate and undergraduate students will be trained. The project team will construct a cloud-based data dissemination system. Scientific results from the project will be exhibited locally and nationally/internationally at conferences and public venues.

CRCNS-specific criteria: (1) *Quality and value of collaboration:* The PI and Co-PIs have complementary expertise in computational neuroscience (Choe, Li), high-performance computing (Li), hardware circuit design (Li), behavioral neuroscience (Smotherman), electrophysiology (Smotherman), neuroanatomy (molecular labeling; Winzer-Serhan), and high-resolution 3D microscopy instrumentation and data analysis (Choe). (2) *New combinations:* PI Choe and Co-PI Li just started collaborating on hardware implementations of neural network models [140]. Co-PI Smotherman and collaborating site's PI Winzer-Serhan are new members of the research team. Previous approach by the PI did not include behavior, electrophysiology, or molecular techniques provided by

these two new members. (3) *Efficient/effective coordination*: All investigators are located in College Station, and a detailed coordination plan is presented at the end of the project description. (4) *High-quality resources*: The correlated behavioral, anatomical, computational, and physiological data resulting from this work will serve as an invaluable resource for the cross-modality research community. The proposed online data dissemination platform is expected to have a high impact. (5) *Unique research experience for students*: Students will be recruited from the computer science, electrical engineering, biology, and neuroscience departments. Weekly meetings and frequent lab visits will provide a unique collaborative research experience. (6) *Clinical/technological applications*: New understanding of common computational principles underlying vision and touch can lead to the development of more effective sensory-substitution devices for the visually impaired (e.g., [3, 51]). Furthermore, the findings can help develop new tactile feedback mechanisms for desktop and mobile computing.

B Background

In this section, we will look at existing works on the visual and tactile processing of texture (Fig. 1).



Figure 1: **Nature of Texture.** A typical texture segmentation task is shown in (a), with its constituent textures in (b) and (c). However, the traditional texture segmentation task is non-existent in a 3D, tactile context as shown in (d) since the two objects (tree trunk and stone) are spatially separated and readily detectable by the sense of touch (the white square marks the texture shown in (a)).

B.1 Visual Perception of Texture

There are many computational methods for texture modeling and processing [6, 7, 32, 45, 48, 49, 50, 66, 122]. These methods employ a wide range of techniques, but they are all based on the implicit assumption that texture is fundamentally a visual property. Hence, most of these methods are based on the use of the Gabor filter, a model of the visual cortical receptive field (see, e.g., [10, 35, 92, 137]). Various models and theories link Gabor-like receptive fields to the statistics of natural scenes [8, 18, 42, 82, 91, 99, 100].

There are more modality-neutral, statistical approaches to texture using second-order statistics [7], Bayesian approaches [12, 142], parametric models [98], generative models [40], texton-based [68, 119], Markov Random Fields (MRF, [70, 118]), and generalizations of the approach [143]. However, the main insights driving these models are deeply rooted in vision.

Visual texture research is mostly based on primate data, however, recent increase in mouse vision research [5] provides a solid ground for our proposed work. Although texture processing has not been demonstrated in mouse vision, the discovery of orientation selectivity in the mouse visual cortex [88], together with the effectiveness of oriented Gabor-like receptive fields in texture processing, suggest that texture discrimination is highly feasible in mouse vision.

B.2 Tactile Perception of Texture

Although computational research on texture has focused more on vision, texture is more immediately a surface property (see e.g., [39, 87, 89] and Fig. 1).

Interestingly, the basic functional organization of the somatosensory system (especially area 3b, the hand area in macaque monkeys) exhibits a close resemblance to that of the visual system,

including the receptive field characteristics and topological mapping of the sensory field [9, 27, 29, 46] and coding mechanisms for touch [136] in the primate finger, while some key differences exist, such as the dynamic component based on finger scanning-direction [30], indicating the importance of active sensing (Fig. 2b).

For rodents, there is an extensive body of work on the whisker-barrel system for texture discrimination [28, 44, 106, 120, 125]. As in the macaque, active sensing is utilized (whisking) in the rodents for texture processing [81]. There is an increasing interest to explore texture and tactile sensation in the rodent fore- and hind-paws, establishing a basis for direct comparison with primate tactile research (area 3b for touch sense in the finger) [25, 34, 34, 71, 123]. Note that in most research on rodents, textures used as stimuli are rather rudimentary, e.g., sand papers of various roughness, or simple groove patterns with different depth and spacing.

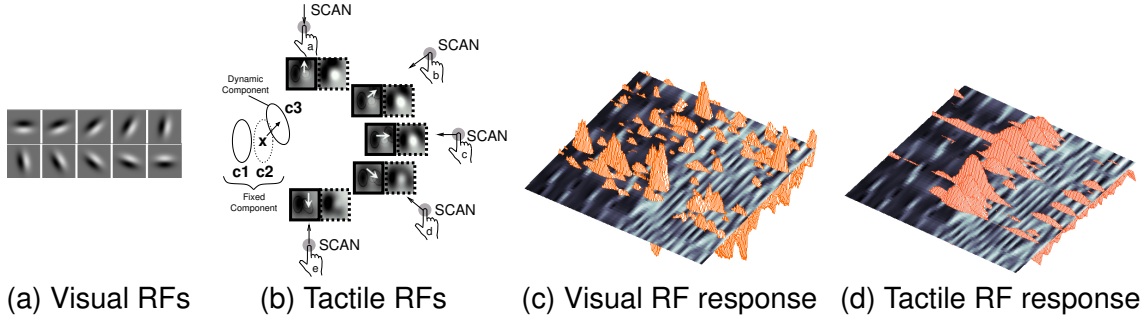


Figure 2: Visual Receptive Fields and Tactile Receptive Fields and Their Responses. (a) Visual receptive fields (RFs) have a oriented Gabor-like pattern. (b) Tactile RFs are similar to visual RFs (e.g., C1 and C2) except for a dynamic inhibitory component (marked C3) whose position relative to the fixed components C1 and C2 changes, centered at “X”, shifting to the opposite direction of the finger scanning direction Adapted from DiCarlo and Johnson [29]. (c) Visual RF model’s and (d) tactile RF model’s responses on a texture with a boundary in the middle is shown in 3D. The tactile RF response has a more prominent hump near the texture boundary than that of the visual RF. Adapted from Bai et al. [4] (PI’s work).

C Prior Work

In this section, we will discuss our computational works on visual vs. tactile texture processing, our whole brain imaging work, and results from prior NSF support.

C.1 Use of Tactile vs. Visual Receptive Fields in Texture Processing

In our prior work [4] we tested the computational power of visual receptive fields (VRFs) and tactile receptive fields (TRFs) when applied to texture boundary detection (Fig. 2). The main hypothesis was that texture is more intimately related with the tactile modality, so that texture images pre-processed with the TRF model would show higher performance than with the VRF model. Our computational experiments validated this hypothesis, where TRF-based method yielded higher texture segmentation performance compared to VRF-based (Fig. 3). For this work, we received the **Best Scientific Paper Award** at the International Conference on Pattern Recognition in 2008.

C.2 Computational Model of Cortical Development: Texture vs. Natural Scene

Building up further on [4], we explored the link between texture-like stimuli and the tactile modality from a developmental point of view, through computer simulations of cortical RF formation [94]. As discussed in the background, natural stimulus statistics and RF patterns are closely related [8, 18, 42, 82, 91, 99, 100]. Based on this, in [94], we tested the hypothesis that visual RFs take their

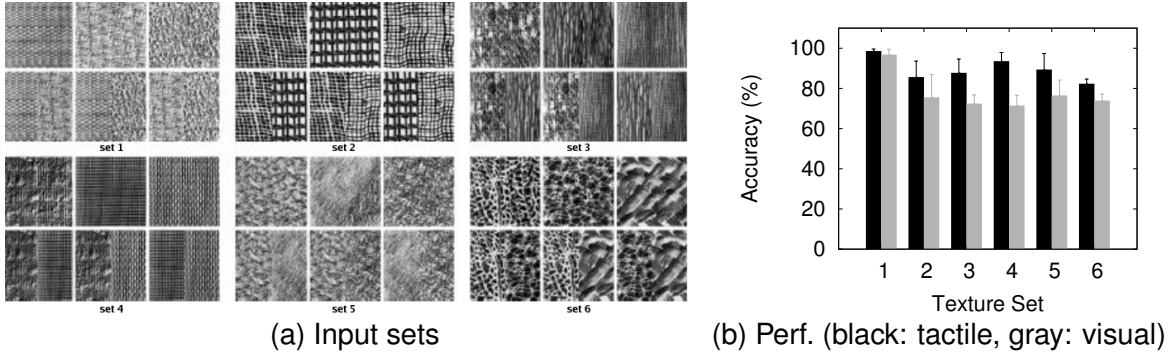


Figure 3: Texture Input Sets and Performance Comparison. (a) Six texture sets used in the boundary detection experiment are shown. In each set, the top row shows the no-boundary condition, and the bottom row the boundary condition. (b) Boundary detection performance (per cent correct) by tactile-receptive-field-based vs. visual-receptive-field-based representations is shown. All cases except for texture set 1, the differences were statistically significant. From [4] (PI's work).

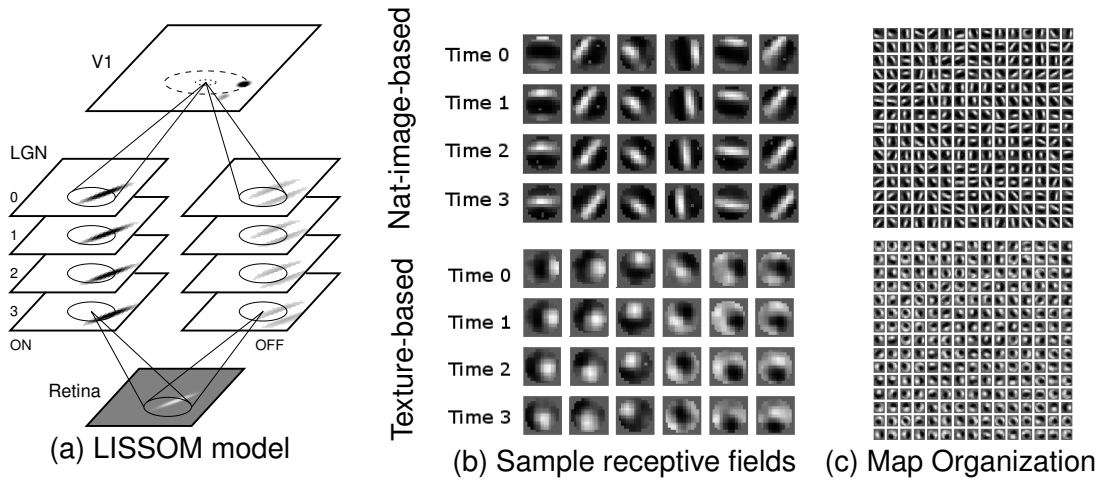


Figure 4: Preliminary Cortical Development Results (Simulation). (a) The same model trained for (b)-(c) [82]. Activity propagates from the bottom (input surface) to the top (cortex). There are multiple time-lagged maps in the thalamus to model dynamic receptive fields. (b) Self-organized receptive fields. Top: trained with natural scene input, shows visual-like receptive fields. Bottom: trained with texture, shows tactile-like receptive fields. Each cortical neuron (in each column), is associated with 4 frames with different time lag. (c) The organization of the map is shown Top: natural-scene-trained. Bottom: texture-trained. Adapted from Park et al. [95] (PI's work).

shape based on natural-scene-like stimulus statistics while tactile RFs form based on texture-like stimulus statistics. We used a general cortical development algorithm based on self-organization called LISSOM (Laterally Interconnected Synergistically Self-Organizing Maps; prior work by the PI Choe [18, 82]; Fig. 4a). Our main finding was that natural-scene-like inputs lead to visual RF-like patterns, while texture-like inputs lead to tactile RF-like patterns (Fig. 4b&c). This work was recognized with the **Best Student Paper Award** at the IEEE Symposium on Computational Intelligence for Multimedia Signal and Vision Processing in 2009.

C.3 Whole Brain Imaging with the Knife-Edge Scanning Microscope

The Knife-Edge Scanning Microscope (KESM, US patent #6,744,572) [13, 58, 76, 77, 78, 79] has been designed at Texas A&M University (TAMU) in recent years with support from the National

Science Foundation (MRI award #0079874; McCormick, PI), Texas Higher Education Coordinating Board (ATP award #000512-0146-2001; Keyser, PI), and the National Institute of Neurological Disorders and Stroke (Award #1R01-NS54252; Choe, PI). The instrument, shown in Fig. 5a, is capable of scanning a complete mouse brain ($\sim 310 \text{ mm}^3$) at 300 nm sampling resolution within 100 hours when scanning in full production mode. The basic operation of KESM is shown in Fig. 5b. A white light source illuminates the rear of the diamond knife, and in turn illuminates the brain tissue at the leading edge of the diamond knife with a strip of intense illumination reflected from the beveled knife-edge. The microscope objective, aligned perpendicular to the top facet of the knife, images the transmitted light. A high-sensitivity line-scan camera repeatedly samples the newly cut thin section, imaging a region 20 μm along the length of the tissue ribbon and just beyond the knife-edge, prior to subsequent deformation of the tissue ribbon after imaging. See Fig. 6 for imaging results (whole mouse brain stained in Golgi).

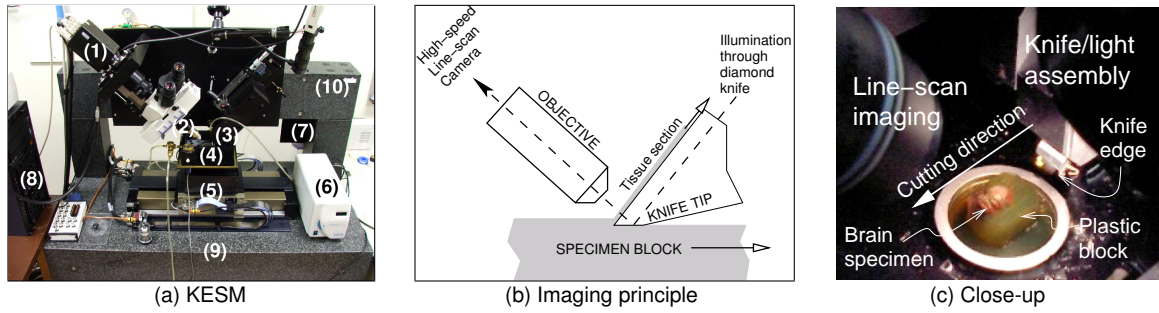


Figure 5: **The Knife-Edge Scanning Microscope (KESM 1.0).** (a) Photo of the KESM 1.0 instrument showing (1) high-speed line-scan camera, (2) microscope objective, (3) diamond knife assembly and light collimator, (4) specimen tank (for water immersion imaging), (5) three-axis precision air-bearing stage, (6) white-light microscope illuminator, (7) water pump (in the back) for the removal of sectioned tissue, (8) PC server for stage control and image acquisition, (9) granite base, and (10) granite bridge. (b) Specimen undergoing sectioning by knife-edge scanner (thickness of section is not drawn to scale). (c) Close-up photo of the line-scan/microscope assembly and the knife/illumination (knife and objective raised to show the brain specimen). Adapted from [24] (PI's work).

C.4 Results from Prior NSF Support (CRCNS Data Sharing)

One of the PI Choe's two CRCNS data sharing grants will be discussed below. **(1) NSF award number, amount, and period of support:** #0905041, \$114,024, 09/01/2009–08/31/2012. **(2) Title of the project:** CRCNS data sharing: Whole Mouse Brain Neuronal Morphology and Neurovasculature Browser. **(3) Summary of results.** **(3-1) Intellectual merit:** The project developed a novel in-browser visualization method for large multiscale 3D microscopy data sets. The technique enabled real-time navigation and browsing of TBs of 3D microscopy data using only a standard desktop computer or even a smartphone/tablet. The high quality mouse brain data from the Knife-Edge Scanning Microscope we are serving on our data sharing platform is of high scientific value, and the tool allowed us to gain unprecedented insights into the organization of the brain at cellular level of detail. The resource is also freely available to the neuroscience research community and the general public, thus its scientific impact is potentially great. **(3-2) Broader impacts:** *Data and code dissemination:* Our main research product is the KESM Brain Atlas that is currently serving data from four mouse brains (two Golgi-stained, one Nissl-stained, and one India-ink-stained). The web site is interactive and is publicly available (Fig. 14c&d). Our atlasing code is also available on SourceForge. *Education:* As part of the two back-to-back grants, we

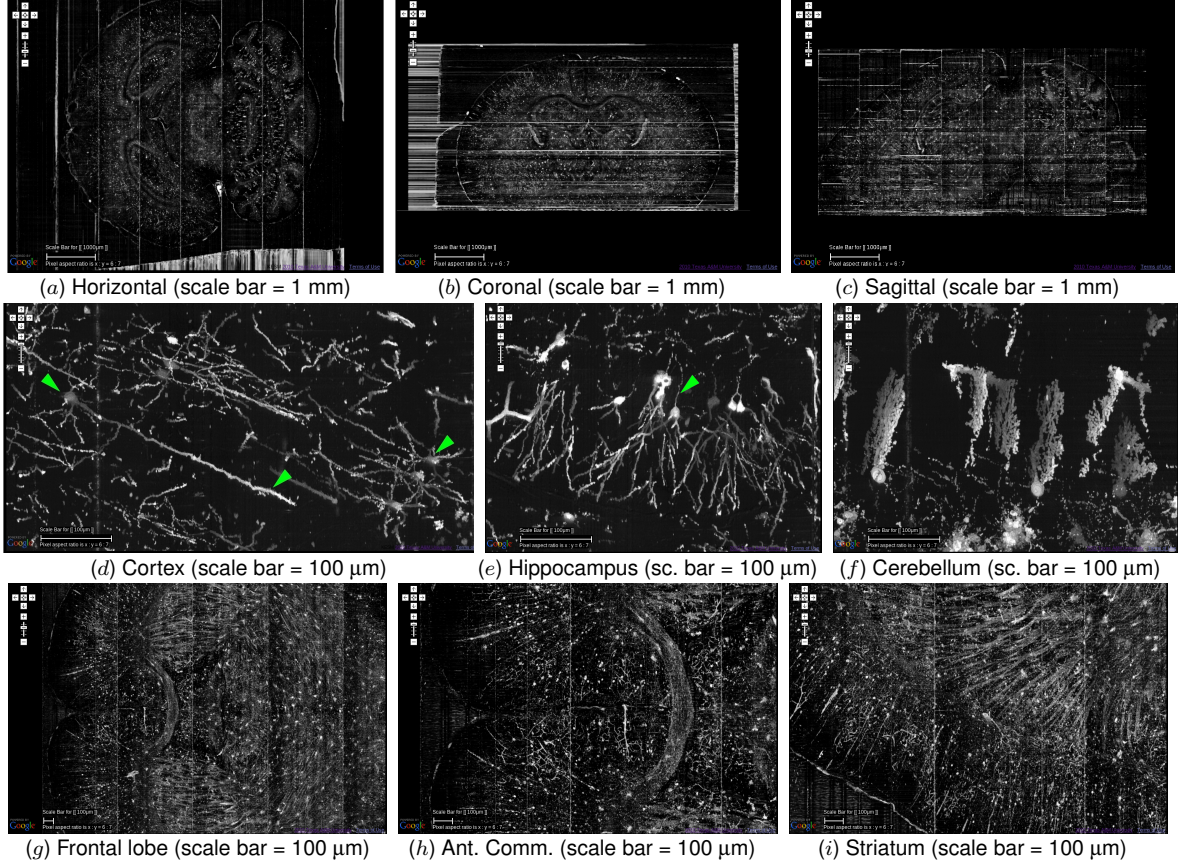


Figure 6: KESM Golgi Data. (a)–(c) Macro-scale views of the KESM Golgi data. (d)–(f) Close-up, showing morphological details of neurons. Arrows (from left to right): pyramidal cell body and apical dendrite. Spiny stellate cells. Hippocampal neuron's axon. (g)–(i) Mid-scale view showing major fiber pathways. Adapted from [24] (PI's work).

trained 1 Ph.D. student, 9 M.S. students, and 7 undergraduate students (4: NSF REU, 3: other funding). See publications below. *Outreach:* Our data and technology were featured in San Francisco Exploratorium's exhibit titled "New Exhibition on Understanding, Influencing Brain Activity", which ran from 1/31/2015–3/1/2015 (Fig. 6&14b). *Tutorials, workshops, and exhibits:* To advertise our work and broaden the user base we ran a tutorial (International Joint Conference on Neural Networks, 2013, Dallas, TX), organized a workshop (Computational Neuroscience meeting, 2010, San Antonio, TX), and three exhibits (Society for Neuroscience, 2011 [Washington, DC], 2012 [New Orleans, LA], and 2014 [Washington, DC]). **(4) Publications.** 6 Conference proceedings (full papers): [16, 57, 60, 74, 113, 139]. 6 Abstracts: [14, 15, 19, 56, 111, 112]. 3 Journals: [17, 24, 75]. 1 Ph.D. dissertation: [110]. 9 M.S. thesis: [23, 31, 53, 59, 84, 108, 109, 133, 138] (note: not all M.S. students were funded by the NSF grant, although the topics covered were in line with the two projects). **(5) Evidence of research products and their availability.** *Online Brain Atlases:* Both brain atlases are currently hosted online, open to the general public (4,727 visitors since 2012: Fig. 14c). The atlase is fully functional, serving whole mouse brain neuronal (Golgi stain and Nissl stain) and vascular (India ink) data. All servers are locally maintained at the PI's lab, with world-wide access. *Data shipping:* We are also shipping hard drives containing data to those who request the data: Johns Hopkins University (Open Connectome project, Joshua Vogelstein); University of California, San Francisco (Nicolas Pannetier); Kettering University (Jaerock

Kwon); King Abdullah University of Science and Technology (Markus Hadwiger); and Louisiana State University (William Donahue).

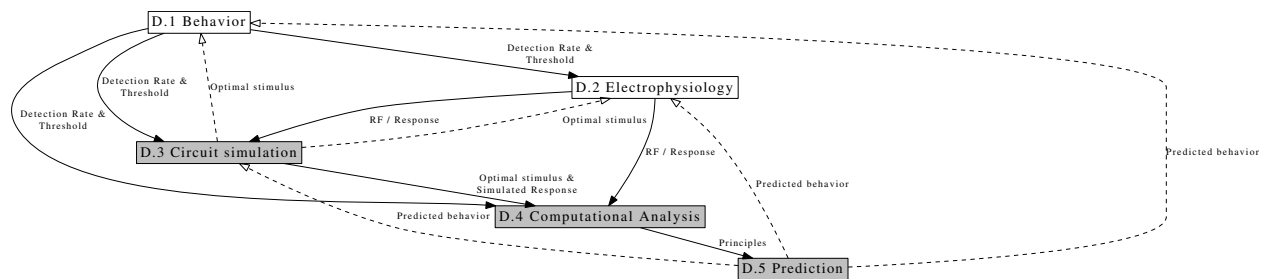
Co-PI Li has also been funded by NSF. **(1) NSF award number, amount, and period of support:** CCF-1117660, \$225,000, 8/1/2011-7/31/2014, **(2) Title of project:** Integrated Verification, Built-in Self-test and Tuning for Digitally-Intensive Analog Systems, PI: P. Li (collaboration with C. Myers/U. of Utah). **(3) Summary of results.** **(3-1) Intellectual Merit:** This work developed a number of methods for verification and test of digitally-intensive analog ICs: fast formal verification techniques accelerated with simulation assistance, Bayesian inference, and parallelization [63, 134, 135], modeling and partitioning techniques to speed up digitally-intensive analog IC verification [65], and machine learning-based algorithms for probabilistic analog design property checking and failure diagnosis [62, 64, 85, 86]. **(3-2) Broader Impacts:** Several students have been trained. One Ph. D. student graduated and joined the Intel Research. Another Ph.D. student interned at Texas Instruments working on analog verification twice and will join TI as a full-time employee. This work has been disseminated through graduate courses, publications and the interactions with Intel, Freescale and TI. **(4) Publications.** Two journal papers [64, 135], and seven conference papers [62, 63, 65, 65, 85, 86, 134] have been published.

Co-PI Smotherman is currently supported by an active NSF grant. **(1) NSF award number, amount, and period of support:** IOS-1354381, \$660,000, 8/15/2014–7/31/2017. PI: Smotherman. **(2) Title of project:** Networking Strategies used by Bats to Improve Social Sonar. **(3) Summary of results.** **(3-1) Intellectual Merit:** Explaining how bats minimize interfering with one other's sonar while flying in dense swarms or within noisy crowded roosts may help improve a wide range of artificial sensing and wireless communications systems. **(3-2) Broader Impacts:** In partnership with local science teachers, this project will create an inquiry-based dual language (Spanish/English) teaching website that will offer access for 5th/6th grade science classes to remotely interact with live animals. **(4) Publications.** This project started just over a year ago, so there is no publication yet.

Collaborating site's PI Winzer-Serhan has been primarily funded by the National Institutes of Health, thus she does not have prior NSF support.

D Research Plan

The road map of the project below shows how different tasks will feed into each other to “close the loop” between computational modeling (gray boxes) and experimental work (white boxes). Edge labels indicate major outcome from each task. Dashed arrows show feedback loops.



D.1 Behavioral Characterization of Visual vs. Tactile Texture Discrimination

Research question(s): Can the mouse be trained to distinguish texture thorough both vision and touch?: (1) uniform texture vs. mixed texture, and (2) same texture vs. different texture?

We will train mice in two-alternative forced choice tasks to establish that they can discriminate texture through both vision and touch (with its paws). It is already known that rodents can dis-

criminate different visual patterns [126] (mice) and rudimentary tactile texture with their whiskers [120, 125] (rats) and paws [71] (mice). In our project, we will extend the behavioral analysis to more complex texture patterns, both for vision and touch in mice.

We will use the water restriction method to motivate learning. Water will be restricted to 1 ml/day for 10 days, followed by training through operant conditioning with water as reward (see [37] for details). Mice will be trained in a T-maze to discriminate between different textures, both in vision (2D) and touch (3D). Water reward will be given at the arm for the correct choice. The behavior will be recorded as a video with a digital camera and the dwell time at the visual/tactile stimulus cue, time-points when the animal enters each arm of the T-maze, and time points of licking will be recorded.

For visual textures we will start with low spatial frequency inputs (to account for poor visual acuity in the mouse), and gradually introduce textures with higher spatial frequency components. For touch, initially, we will use 3D printed textures for the forepaw, and subsequently use a tactile array to generate dynamic texture surfaces. The two alternative choices will be either

- Set 1: Choice 1 = uniform vs. Choice 2 = mixed texture, or
- Set 2: Choice 1 = same vs. Choice 2 = different texture, given two successive patterns.

See Fig. 7 below. The specific texture patterns will be determined as we calibrate the experimental set up, and different texture combinations will be used for training the general concept of texture. The visual or tactile cues will be placed at the entrance of the T-maze, and reward will be administered on the correct side of the T-maze. For the tactile stimulus, a slightly elevated platform with texture on top will be used so that the forepaw will touch the texture first (Fig. 7c&d). This will also prevent the use of whiskers.

Success rates under varying stimulus conditions will be measured. The information will be analyzed to derive detection threshold.

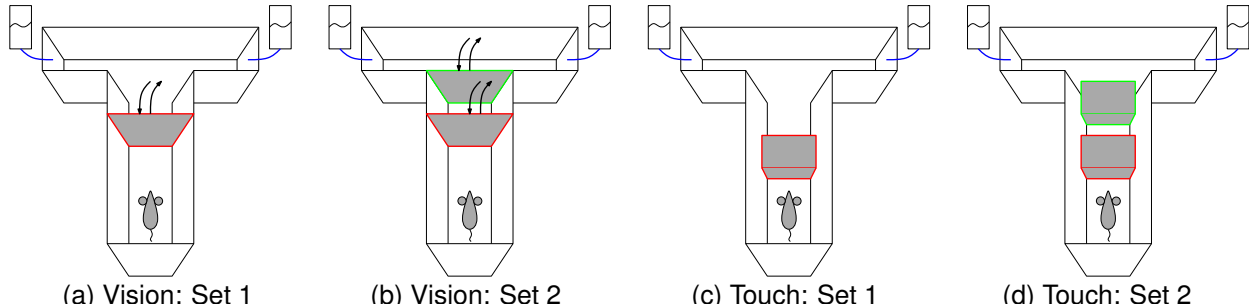


Figure 7: Behavioral Paradigm. Different T-maze configurations are shown for different combinations of modalities and alternative choice sets. For (a) and (b), the visual stimuli will be either shown on a screen at the end of the hallway or inserted with card boards (and removed). Set 1: uniform or mixed texture. Set 2: same or different textures. See text for details.

D.2 Electrophysiological Measures of Visual vs. Tactile Texture Discrimination

Research question(s): (1) What is the response property of layer 4 neurons (single and population) in mouse visual and somatosensory cortex, in response to textural input? (2) How are their receptive fields structured?

Task 1: Create high-resolution three-dimensional receptive field (RF) maps of neurons in visual and somatosensory cortex in anesthetized mice. For visual receptive field studies, urethane-anesthetized mice will be positioned in a custom-built stereotaxic apparatus facing a translucent spherical dome projection screen (27.5 cm diameter) centered on one eye. Eyelids are

held open with loose sutures, pupils dilated with a solution of 1% topicalamide and 2.5% phenylephrine HCl , and the cornea protected with ophthalmic ointment. Visual stimuli are projected from a PC onto the screen. Initial characterization of individual neuron receptive fields will be done with annular, slit and edge stimuli varying in size, orientations, and contrast intensities. Neuronal response characteristics will be recorded with glass micropipettes positioned in layers 2/3 and 4 of V1 and neighboring extrastriate visual cortex. Areas found to have spatial frequency preferences similar to those contained within the complex textural stimuli will receive the greatest attention.

For tactile receptive field studies, urethane-anesthetized mice will be positioned in a custom-built stereotaxic apparatus equipped with digitally-manipulated 3D electromagnetic probe positioned under the forepaw. To quantify response characteristics and create a detailed map of cutaneous RFs from glabrous skin of the forepaw, we will record extracellular responses (multi-unit recordings) using glass microelectrodes while applying sequences of vibrotactile stimuli to the ventral surface of the forepaw. Layer 4 pyramidal neurons will be targeted based upon recording depth and spontaneous firing rates. The single point probe is moved in 100 μ m steps rostrocaudally and mediolaterally around the paw and at each set of coordinates the vertical distance and force of the probe is varied following a pseudorandom sequence optimized to rapidly and efficiently map the neurons RF based on changes in spike rates at each site. Stimulus durations are 10 ms delivered at 1 Hz and averaged over 30 repetitions. Each receptive field requires approximately 24 sites, iteratively controlled by the experimenter. 3D RF maps fitted to the paw contour are generated post-hoc using custom MATLAB routines.

Task 2: Assess response characteristics of visual and somatosensory cortical neurons to complex 2D and 3D texture stimuli. Animals are prepared as in task 1 and neurons are recorded similarly in urethane-anesthetized mice. For visual cortex, a series of visual textural patterns (2D) will be projected onto the screen. For somatosensory cortex the forepaw is stimulated by an identical series of different 3D-printed surfaces differing in textural patterns. For both sensory modalities each pattern is gradually refined in its design to best evaluate how the neurons receptive field properties change when neighboring receptive fields are simultaneously manipulated in specific textural patterns (this step requires a closed loop through §D.3). The patterns are designed to accommodate direct comparisons to prior results defining how the visual system processes textural cues.

Task 3: Characterize the RFs and ensemble firing patterns of visual and somatosensory cortex in response to common textural stimuli using a chronically-implanted wireless (TBSI) microelectrode array (8-channel surface probe, Neuronexus) in awake behaving animals. Under isoflurane anesthesia the microelectrode array will be stereotactically positioned unilaterally over either V1 and neighboring extrastriate visual areas or over the forepaw region of somatosensory cortex, with electrode tips projecting to an approximate depth of 150-250 μ m, and the mouse allowed to heal for 5–7 days before beginning behavioral trials. Mice will be trained to discriminate between visual and tactile textures (same stimuli as in tasks 1 and 2) in the T-maze and during experimental trials neuronal activity will be assessed in relation to the time-points when the animal enters each arm of the T-maze. For the tactile (substrate) stimuli neuronal activity will be assessed relative to when the animals forepaw makes contact with the substrate to create peri-event time histograms (PETHs). PETHs will be compared across texture stimuli, exploiting cross-correlation analyses across different stimulus design features to extrapolate single unit RFs in awake, behaving animals. Data analyses and modeling will test the null hypothesis that RF features derived from texture discrimination tasks can be modeled by a similar set of rules guiding linear integration of single unit RF features in both visual and somatosensory cortex as derived from tasks 1 and 2.

D.3 Anatomically Correct Large-Scale Circuit Reconstruction and Simulation

Research question(s): (1) What is the role of horizontal connections in the mouse visual and somatosensory cortex for texture encoding and discrimination? (2) What kind of features in texture stimuli lead to more discriminable layer 4 response patterns?

Overview: Characterizing electrophysiological behaviors of the cells and building biologically realistic models for the visual and somatosensory cortices is an integrated part of the proposed work. To this end, biophysically detailed neuronal models (e.g. Hodgkin-Huxley type models [41]) will be adopted for modeling various cell types in the visual and the somatosensory cortices. We will take a complementary approach to neuronal cell modeling wherein a combination of our own morphological and biophysical data and published experimental data are used. The KESM data, when used in conjunction of our automated 3D reconstruction algorithms [38, 73, 130, 131, 132] and available tools such as FARSIGHT (University of Houston) [67] or Vaa3D (Allen Institute) [96], offer a promising opportunity to build a large set of biophysically realistic neuronal models using reconstructed morphological data (Fig. 6). The accuracy of cell modeling (hence the accuracy of behavioral characterization) is a key enabler. To achieve this goal, each cell type will be modeled with high-precision using a large number of compartments (on the order of hundreds per neuron). By utilizing the connectivity data obtained from the KESM and public domain databases (e.g. Allen Mouse Connectivity Atlas [1]; Fig. 8), we will further construct biophysically realistic models for the visual and somatosensory cortices. The Allen data can be used as a connection probability distribution, while the KESM dendritic (and local projection) data can provide detailed postsynaptic target locations. Based on these data, we will adopt methods developed by [52, 72] for the circuit reconstruction. The resulting circuit will provide a starting point for computer simulation based analysis of texture processing. Note that due to the limited scope of this project, an extensive simulations like those of the European Human Brain Project [72] is not possible, and also that our proposed method uses real anatomical data, not synthetic circuits.

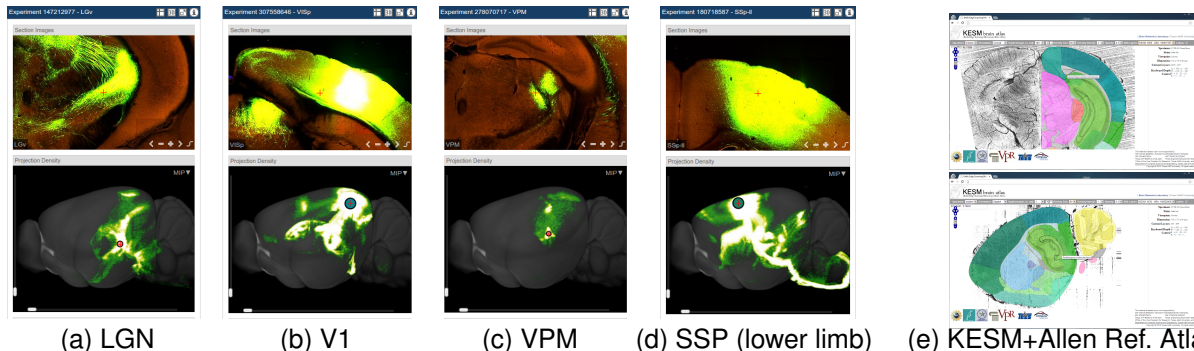


Figure 8: **Allen Mouse Connectivity Atlas.** (a)–(d) Sample connections from the visual and somatosensory areas of the cortex and thalamus from the Allen Mouse Connectivity Atlas are shown [1]. LGN: lateral geniculate nucleus. V1: primary visual cortex. VPM: ventral posterior medial nucleus of the thalamus. SSP: Primary somatosensory area. (e) Preliminary work (PI's lab): KESM India Ink data registered to the Allen Reference Atlas (Top: coronal; Bottom: sagittal).

Task 1: KESM imaging. Collaborating site's PI Winzer-Serhan will be responsible for specimen preparation for KESM imaging. The goal is to digitally reconstructed three-dimensional model of inhibitory and excitatory neurons and their local circuit connections, in forepaw somatosensory and primary visual cortices (layers 2 through 4). (1) *Neuronal morphology and cell type.* Young adult mice ($n=6$ /marker) will be perfused with 4% paraformaldehyde, their brains collected and cut into

blocks containing the forepaw somatosensory and visual cortices. The tissue will be processed for immunohistochemistry using cell specific primary antibodies for NeuN (all neurons) and for GAD67 (GABAergic inhibitory interneurons; Fig. 9a) followed by a biotinylated secondary antibody, and will be visualized with an avidin-peroxidase diaminobenzidine (DAB) reaction enhanced with nickel and cobalt to generate a permanent black reaction product. After staining, the tissue will be embedded in epon or araldite for cutting using the KESM (see our protocol paper for details [17]) and subsequently sectioned and imaged with the KESM (for fluorescence imaging with KESM, we will use our second generation KESM built by 3Scan [a startup company located in San Francisco]). Pyramidal and inhibitory cell types will be identified based on their different morphologies and layer locations, which has been used in the past, and can be applied to the somatosensory and visual cortices [2, 26, 47]. The results from the KESM will be validated using standard light microscopy and immunofluorescence confocal microscopy after immuno-histochemistry staining in slices using optical disectors [11, 36, 124] and Stereo Investigator software (StereoInvestigator 7.0, Microbrightfield). (2) *Local circuits*. Specific dendritic morphologies and axonal projections need to be imaged to determine local circuits. However it is known that morphologically similar neurons can have differences in their connectivity [54, 107]. We will fill hundreds of neurons in the visual and somatosensory cortex with biocytin (Fig. 9b), and subsequently conjugated with avidin-biotinylated peroxidase and visualization with DAB for imaging with the KESM. The same embedding procedure will be used as above [17]. In order to reconstruct inputs from thalamic neurons to visual and sensory cortical receptive fields, anterograde tracer experiments with biotinylated dextran amine (BDA 10k, Molecular Probes) will be conducted [101]. The tracer will be injected into the ventral postrolateral nucleus (VPL) which projects to somatosensory cortex, and into the lateral geniculate nucleus (LGN) which projects to visual cortex. BDA (10 kDa) yields sensitive and detailed labeling of axons and terminals, and can be visualized with an avidin-biotinylated horseradish peroxidase procedure, followed by a metal-enhanced DAB reaction, which allows detection by the KESM. Digital reconstruction of thalamic projections to multiple cell types in individual cortical layers will be done based on the data sets derived from the KESM analysis.

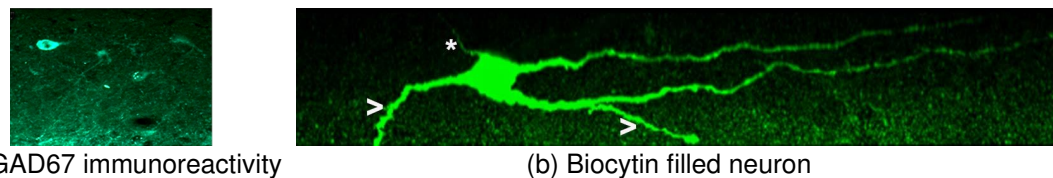


Figure 9: Staining for Cell Type and Connectivity. (a) Fluorescence image of GAD67 immunoreactivity in inhibitory interneurons in the CA1 field of the mouse hippocampus. (b) Biocytin filled neuron in a 300 μ m thick mouse brain section (*: axon; >: dendrites): z-stack imaging with confocal fluorescent microscope. Preliminary work from collaborating site PI Winzer-Serhan's lab.

Task2: Computational simulation. Co-PI Li has extensive experience in biophysically based modeling of neuronal networks, parallel numerical techniques for large-scale simulation of brain models, and computational modeling of epilepsy, and development of parallel neural network simulation tools on multi-core shared memory machines, massively parallel graphic processors and supercomputers [43, 121, 127, 128, 129, 141]. In particular, his lab has developed a large-scale biophysically realistic thalamocortical model and an in-house parallel neural network simulator [141]. The model consists of a modeled six-layered cerebral cortex with 70 brain regions and multiple thalamic nuclei connected according to global white fiber imaging data. More than 22 types of neurons are characterized using multi-compartmental Hodgkin-Huxley models based on published experimental data. A number of efficient parallel computational techniques have developed in the dedicated simulator to speed up large-scale dynamic simulation. This simulation environment has

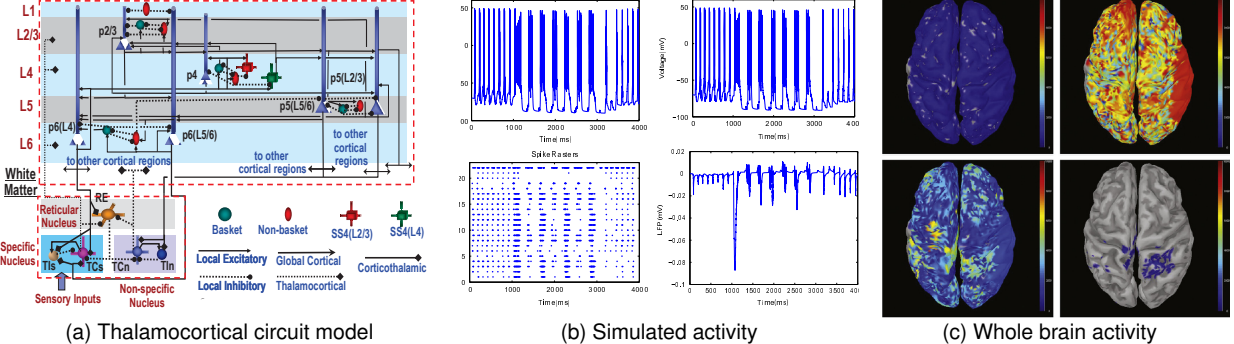


Figure 10: Whole Brain-Scale Simulation. (a) Local circuit model including 6 layers of the cortex and the thalamus. (b) Transition from spindles to epileptic seizure. Top row: membrane potential of two pyramidal cells from the deep layer. Bottom row: spike raster (left) and local field potential (right). (c) Time lapse of layer 4 activity. Top left: at 570 ms (active, delta wave). Top right: at 1190 ms (active, seizure). Bottom left: at 2140 ms (inactive, seizure). Bottom right: at 3700 ms (inactive, delta wave). The simulation was over 70 cortical regions, 1 million neurons and 305 million synapses. Adapted from [141] (Co-PI Li's work).

also been ported to the machines at the Texas A&M Supercomputing Center [43]. This modeling and simulation environment makes it possible to feasibly simulate brain models of more than one million multi-compartmental neurons and hundreds of millions of synapses on a commodity 24-processor server. Such simulations reproduced sigma and delta waves occurring in the early and deep sleep stages, shed light on the role of synaptic characteristics in generating seizures, reveal the firing activities of various cell types (Fig. 10).

In this work, we will conduct large-scale computer simulation of the visual and the somatosensory cortex using multicompartmental neuron models, based on hard anatomical data from the KESM and the Allen Connectivity Atlas. As part of this objective, efficient numerical simulation methods and tools will be developed to allow feasible and efficient simulation of large cortex models. *The resulting simulation will allow us to test a much larger array of texture patterns than we can in behavioral trials and in electrophysiology experiments.* Furthermore, we will conduct artificial lesions to study the role of horizontal connections in texture processing. It is expected that this kind of computational approach will provide deep insights on the computational principles embedded in texture processing and shared across vision and touch.

D.4 Analysis of Data to Derive Common Computational Principles

Research question(s): (1) What are the shared properties in response statistics between visual and somatosensory response to texture stimuli? (2) How does information from neighboring neurons contribute to texture discrimination in vision and touch? (3) Can discriminability of cortical representation of texture reflect behavioral performance?

Task 1: Statistical analysis of cortical response. The first step in finding similarities and differences between visual and tactile texture processing is to compare basic statistics of cortical response to texture. It is well known that visual cortical activity exhibits a power law distribution in response to natural scene stimuli [33]. Can the same be observed in visual cortical and somatosensory cortical responses to texture? If so, what could that suggest regarding shared texture processing principles? Our preliminary computational results indicate that both visual cortex and somatosensory cortex would show response power law when exposed to texture (Fig. 11). To answer these questions, we will compute the response histogram from (1) electrophysiology

data from §D.2 and from (2) our computational simulations §D.3, and compare the distributions using Kullback-Leibler Divergence [55] and their power law exponent. What use can this response power law have? In our earlier work, we showed that when compared to a Gaussian baseline, the power law distribution can be used to detect saliency threshold [61, 102] (Fig. 12). We will further investigate this possibility in texture processing.

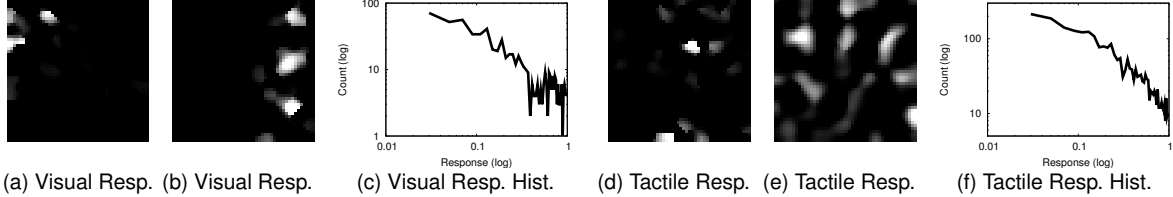


Figure 11: Power Law in Visual vs. Tactile Response (Simulated). Computational simulation results of visual and somatosensory cortex are shown (from the LISSOM simulation in Fig. 4). Typical activation patterns and response histogram for vision (a)–(c) and touch (d)–(f) are shown. The histograms are in log-log scale, exhibiting power law. Adapted from [94] (PI’s work).

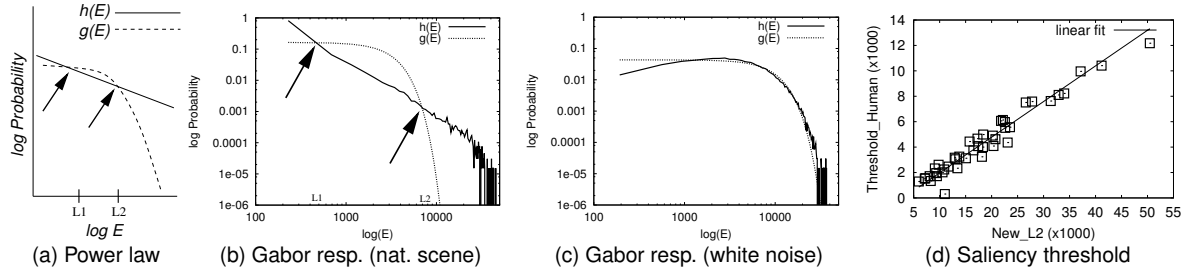


Figure 12: Gabor Response Distribution Analysis for Saliency Detection. (a) Gabor filter response (E) distribution exhibiting a power law property ($h(E)$) is contrasted against a normal distribution with the same variance ($g(E)$), in log-log scale. (b) Response (E) to natural images ($h(E)$) shows a power law distribution. (c) Response to white-noise images ($h(E)$) is close to normal distribution. (d) Response threshold based on the L_2 value (where $h(E) > g(E)$) shows an almost linear fit to human-selected threshold (correl. coeff. $r = 0.98$). Adapted from [102] (PI’s work).

Task 2: Correlating texture discriminability within stimuli vs. discriminability within cortical response. To find the dominant factors for texture representation and to measure discriminability, we will apply kernel Fisher discriminant (KFD) [83] to (1) the raw input and (2) the feature spaces of the cortical responses. KFD is a generalized version of Fisher discriminant analysis (or linear discriminant analysis, LDA) using kernel trick as in support vector machines or kernel principal component analysis [103]. KFD is a good first choice for visualizing high-dimensional data such as the tactile and visual response vectors, and can also be used for classification.

We will also use kernel Isomap [20, 21, 22]. In kernel Isomap Given N objects with each object being represented by an m -dimensional vector \mathbf{x}_i , $i = 1, \dots, N$, the kernel Isomap algorithm finds an implicit mapping which places N points in a low-dimensional space. In contrast to Isomap [115], the kernel Isomap can project novel data points onto the discovered low-dimensional space, as well, through a kernel trick. The kernel Isomap mainly exploits the solution of the additive constant problem, the goal of which is to find an appropriate constant to be added to all dissimilarities (or distances), apart from the self-dissimilarities, that makes the kernel matrix positive semidefinite. Given a distance matrix, we use Dijkstra’s geodesic distances (shortest paths) \mathbf{D} , and calculate the doubly centered kernel matrix as below.

$$\mathbf{K} = -\frac{1}{2}\mathbf{H}\mathbf{D}^2\mathbf{H}, \quad (1)$$

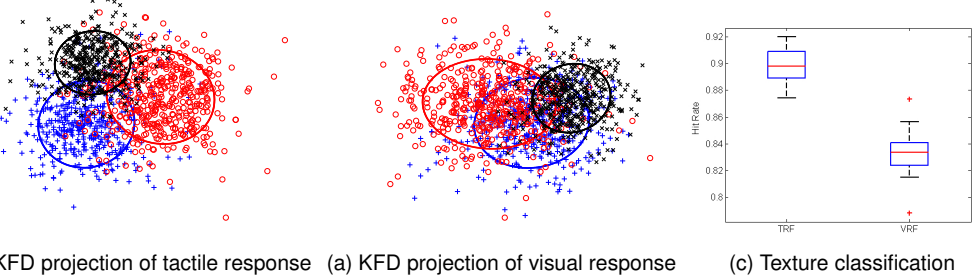


Figure 13: Kernel Fisher Discriminant Analysis of Tactile and Visual Response Vector Space, and Texture Classification. Projections using Kernel Fisher Discriminant analysis of (a) Tactile response and (b) visual response to three texture classes (LISSOM simulation). Ellipses = equidistant traces from each class' mean with 1.5X std. TRF response space is more separable. (c) Texture classification (three classes) based on projection of tactile and visual response vectors onto the first two eigenvectors from KFD show superior performance for the tactile receptive field ($n = 30$, k-NN classifier). The box-and-whisker plot shows the median, top and bottom 25-percentile, standard deviation, and outliers (+). Adapted from [93] (Ph.D. work from PI's lab.)

where $\mathbf{D}^2 = [D_{ij}^2]$ means the element-wise square of the geodesic distance matrix $\mathbf{D} = [D_{ij}]$, \mathbf{H} is the centering matrix, given by $\mathbf{H} = \mathbf{I} - \frac{1}{N}\mathbf{e}_N\mathbf{e}_N^\top$ for $\mathbf{e}_N = [1 \dots 1]^\top \in \mathbb{R}^N$. Then, we make the kernel matrix positive definite by adding a constant, c .

$$\widetilde{\mathbf{K}} = \mathbf{K}(\mathbf{D}^2) + 2c\mathbf{K}(\mathbf{D}) + \frac{1}{2}c^2\mathbf{H}, c = \text{largest eigenvalue of } \begin{bmatrix} \mathbf{0} & 2\mathbf{K}(\mathbf{D}^2) \\ -\mathbf{I} & -4\mathbf{K}(\mathbf{D}) \end{bmatrix}. \quad (2)$$

Eq. (2) implies substituting $\widetilde{\mathbf{D}}$ for \mathbf{D} in Eq. (1), which is given by $\widetilde{D}_{ij} = D_{ij} + c(1 - \delta_{ij})$, which makes the matrix \mathbf{K} positive semi-definite. The term δ_{ij} is the Kronecker delta. Finally, projection mapping \mathbf{Y} is obtained by eigen-decomposition of $\widetilde{\mathbf{K}} = \mathbf{V}\Lambda\mathbf{V}^\top$: $\mathbf{Y} = \mathbf{V}\Lambda^{\frac{1}{2}}$. The projection for novel data points is similar as in kernel PCA and is described in [21]. These methods are expected to quantitatively evaluate the discriminability of the tactile vs. the visual representation of texture.

We will apply KFD and kernel Isomap to the responses of tactile and visual cortices (both experimental and simulated) on texture inputs from several texture classes (similar to the Brodatz set and natural textures). Fig. 13a&b shows preliminary results using KFD. The figure shows that the tactile responses give clusters that are more separable across texture classes than those based on visual responses. We will then perform classification using the projections on the KFD and Kernel Isomap basis functions. Standard classifiers such as support vector machines (in this case, the multi-class variant) will be used. Fig. 13c shows our preliminary results (with k-NN classifier in this case) where tactile representation exhibits higher classification performance compared to visual representation.

Task 3: Deriving computational principles. Malik and Perona [69] proposed that preattentive texture processing consists of three computational components: (1) convolution with even-symmetric filters followed by half-wave rectification, (2) lateral inhibition, and (3) boundary detection using odd-symmetric mechanisms. First, we will check if all of these principles hold for experimental and computational data from our project, for both vision and touch. Next, we will check if (4) inclusion of dynamic response (as opposed to one-shot, static response) makes texture more discriminable. For all of the components above, we will vary simulation parameters (such as horizontal connection weight, delay, etc.), stimulus dimensions (texton, scale, distribution, repeat direction, etc.), and neuronal connectivity (artificial lesion) to probe further for common and distinct computational principles of texture representation and processing.

D.5 Predictions from the computational principles and experimental validation

Research question(s): (1) Can results from artificial lesion studies or noise studies on the computational simulation be replicated experimentally? (2) Can measured discriminability in simulated cortical response match behavioral performance?

Since concrete predictions would require a working computational model fitted to data resulting from this project, instead of offering predictions, we will discuss specific procedures we will follow to generate and test the predictions. Basically we will look into predicted outcomes when circuits are altered: weights, connectivity, cell type. We will also check predicted outcomes when the stimuli are varied systematically. Finally, we will validate the predictions through behavioral and electrophysiological measures described in §D.1 and §D.2. Example predictions: (1) Weaker lateral inhibition would lead to weaker texture discriminability, and thus poorer behavioral performance. (2) Longer (as opposed to instantaneous) cortical response would lead to better performance.

E Broader Impacts of the Proposed Work

(1) *Education:* We will train four graduate students to become experts in computational neuroscience. We will also train undergraduate students through the NSF Research Experience for Undergraduates (REU) program (see budget request and REU request document). The data from this project are expected to serve as a rich resource for educational use. The proposed online data dissemination platform is expected to be used at graduate and undergraduate-level courses taught by the PI and Co-PIs.

(2) *Outreach:* We will also organize exhibits and tutorials at biology conferences to broaden the user base and adoption of our data and online data dissemination platform (PI Choe has extensive experience with organizing exhibits, symposia, workshops, and tutorials). Our work has also been featured in San Francisco's Exploratorium exhibit (2015 spring), and we will pursue similar opportunities for public outreach. See Fig. 14a&b.

(3) *Data and code dissemination:* We will host our own data on a cloud-based portal (based on our KESM Brain Atlas framework; see Fig 14c&d showing access statistics and world-wide visitors), and also ship our data to the CRCNS Data Sharing portal (hosted at University of California, Berkeley; PI: Jeff Teeters and Fritz Sommer [114]). All code for data organization and analysis will be made public on GitHub (utilizing the enterprise license at Texas A&M University).

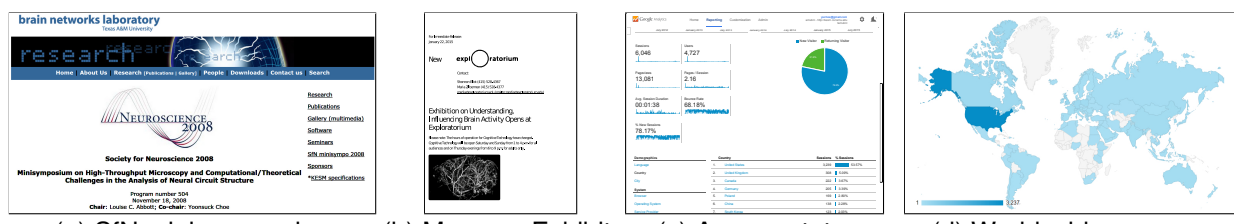


Figure 14: **Broader Impact.** Web page screenshots: (a) 2008 Society for Neuroscience Mini-Symposium on high-throughput imaging. (b) 2015 San Francisco Exploratorium Exhibit on the brain (featuring KESM India ink data at the bottom; exhibit arranged by collaborator 3Scan, located in San Francisco). Google Analytics data on the KESM Brain Atlas: (c) access stats (February 2012 to present: 4,727 visitors, 13,081 page views) and (d) world-wide access plot showing broad world-wide usage. Some screenshots were edited (elements rearranged) to fit the page.

F Management Plan: Please see §G.

G Coordination Plan

G.1 Specific roles of PI/Co-PIs

The table below shows the objectives, timeline, and specific roles of the PI and Co-PIs. Major activities will take place as shown in the table below, but for each task, preparation work will start ahead of the indicated time period.

Table 1: Objectives, Timeline, and Role

Objectives	Year 1	Year 2	Year 3	Lead, Support
Obj. §D.1 Behavior	■■■			Smotherman, Choe
Obj. §D.2 Electrophysiology	■■■	■■■		Smotherman, Li
Obj. §D.3 Circuit simulation	■■■	■■■		Li, Choe, Winzer-S.
Obj. §D.4 Analysis & Computational Principles	■■■	■■■		Choe, Li, Winzer-S.
Obj. §D.5 Predictions and validation		■■■	■■■	Winzer-S., Smotherman
Obj. §E Broader Impact	■■	■■	■■■	Choe, Smotherman

* Each year is divided into Summer, Fall, and Spring Semester.

G.2 Management across institutions/disciplines

1. *General management:* All collaborating departments are reachable within 15 minutes either by walking or driving, greatly facilitating high-quality interaction. PI Choe will be the main organizer and manager for the Texas A&M Engineering Experiment Station side of the project. Collaborating PI Winzer-Serhan will be the main manager for the Texas A&M Health Science Center side.
2. *Financial management:* Both Texas A&M University and Texas A&M University Health Science Center are served by the same sponsored research office (TAMU System Sponsored Research Services, SRS), thus budget and spending will be monitored by a single entity, greatly simplifying management.
3. *Unit (department) management:* For each unit from Computer Science and Engineering, Electrical and Computer Engineering, Biology, and Neuroscience and Experimental Therapeutics, the respective PI/Co-PI will be responsible for the management.
4. *Cross-disciplinary management:* For coordination of management across units and disciplines, the four PI/Co-PIs will have a weekly “faculty only” meeting right after the general weekly meeting including all project personnel (all investigators and students).
5. *Data and document sharing and management:* A cloud-based collaboration platform will be used to archive important data, meta data, documents, procedures, best practices. etc. Texas A&M University has an enterprise license for a broad set of Google services, including Gmail, Google Drive, etc., which we will utilize extensively. For computer code, we will use Texas A&M University’s enterprise license for GitHub, a web-based version control system.

G.3 Coordination mechanisms

1. *Planning meeting:* At the beginning of each semester, we will hold a all-hands meeting to decide on a detailed list of tasks for the semester.
2. *Weekly meeting:* During the semester, we will organize weekly meetings. Each week, we will review the list of tasks for the semester determined during the planning meeting and check

the progress. We will also plan on what to do next the following week as tasks get completed. The weekly meeting time will also be used for project presentations and discussion of latest results in the literature.

3. *Monthly meeting:* We will also organize a monthly social so that project team members can exchange ideas in a more informal setting, which we expect to facilitate interdisciplinary cultural exchange.
4. *Annual workshop:* At the end of each Spring semester, the project team will host an annual workshop, open to the local research community. The workshop will feature invited local speakers and presentations by project personnel. The workshop will include panels to discuss latest results from the project and future directions.

G.4 Budget items

Since both collaborating institutions (Texas A&M Engineering Experiment Station and Texas A&M University Health Science Center) and the four home departments of the PI and Co-PIs are located in College Station, TX, no specific funding is requested for travel, etc. to coordinate in-person meetings.

REFERENCES CITED

- [1] Allen Institute for Brain Science (2012). ALLEN mouse brain connectivity atlas technical white paper: Overview. Technical Report October 2012 v.4, Allen Institute for Brain Science. <Http://connectivity.brain-map.org>.
- [2] Ascoli, G. A., Alonso-Nanclares, L., Anderson, S. A., Barrientos-Piccione, R., Burkhalter, A., Buzsáki, G., Cauli, B., DeFelipe, J., Fairén, A., Feldmeyer, D., Fishell, G., Fregnac, Y., Freund, T. F., Gardner, D., Gardner, E. P., Goldberg, J. H., Helmstaedter, M., Hestrin, S., Karube, F., Kisvárday, Z. F., Lambolez, B., Lewis, D. A., Marin, O., Markram, H., Muñoz, A., Packer, A., Petersen, C. C. H., Rockland, K. S., Rossier, J., Rudy, B., Somogyi, P., Staiger, J. F., Tamas, G., Thomson, A. M., Toledo-Rodriguez, M., Wang, Y., West, D. C., and Yuste, R. (2008). Petilla terminology: nomenclature of features of GABAergic interneurons of the cerebral cortex. *Nature Reviews Neuroscience*, 9:557–568. For the Petilla Interneuron Nomenclature Group (PING).
- [3] Bach-Y-Rita, P., Collins, C. C., Saunders, F. A., White, B., and Scadden, L. (1969). Vision substitution by tactile image projection. 221:963–964.
- [4] Bai, Y. H., Park, C., and Choe, Y. (2008). Relative advantage of touch over vision in the exploration of texture. In *Proceedings of the 19th International Conference on Pattern Recognition (ICPR 2008)*, 1–4, 10.1109/ICPR.2008.4760961. **Best Scientific Paper Award**.
- [5] Baker, M. (2013). Through the eyes of a mouse. *Nature*, 502(7470):156–158.
- [6] Beck, J. (1966). Effect of orientation and of shape similarity on grouping. *Perception and Psychophysics*, 1:300–302.
- [7] Beck, J. (1983). Textural segmentation, second-order statistics and textural elements. *Biological Cybernetics*, 48:125–130.
- [8] Bell, A. J., and Sejnowski, T. J. (1997). The “independent components” of natural scenes are edge filters. *Vision Research*, 37:3327.
- [9] Bensmaia, S., Eenchev, P., Maass III, J. D., Craig, J., and Hsiao, S. (2008). The representation of stimulus orientation in the early stages of somatosensory processing. *Neuroscience*, 28:776–786.
- [10] Bovik, A., Clark, M., and Geisler, W. (1990). Multichannel texture analysis using localized spatial filters. *IEEE Transactions on Pattern Analysis and Machine Intelligence*, 12(1):55–73.
- [11] Butt, S. J., Fuccillo, M., Nery, S., Noctor, S., Kriegstein, A., Corbin, J. G., and Fishell, G. (2005). The temporal and spatial origins of cortical interneurons predict their physiological subtype. *Neuron*, 48(4):591–604.
- [12] Chan, A., and Vasconcelos, N. (2006). Layered dynamic textures. In Weiss, Y., Schölkopf, B., and Platt, J., editors, *Advances in Neural Information Processing Systems 18*, 203–210. Cambridge, MA: MIT Press.
- [13] Choe, Y., Abbott, L. C., Han, D., Huang, P.-S., Keyser, J., Kwon, J., Mayerich, D., Melek, Z., and McCormick, B. H. (2009). Knife-edge scanning microscopy: High-throughput imaging and analysis of massive volumes of biological microstructures. In Rao, A. R., and Cecchi,

G., editors, *High-Throughput Image Reconstruction and Analysis: Intelligent Microscopy Applications*, 11–37. Boston, MA: Artech House.

- [14] Choe, Y., Abbott, L. C., Miller, D. E., Han, D., Yang, H.-F., Chung, J. R., Sung, C., Mayerich, D., Kwon, J., Micheva, K., and Smith, S. J. (2010). Multiscale imaging, analysis, and integration of mouse brain networks. In *Neuroscience Meeting Planner, San Diego, CA: Society for Neuroscience*. Program No. 516.3. Online.
- [15] Choe, Y., Abbott, L. C., Ponte, G., Keyser, J., Kwon, J., Mayerich, D., Miller, D., Han, D., Grimaldi, A. M., Fiorito, G., Edelman, D. B., and McKinstry, J. L. (2010). Charting out the octopus connectome at submicron resolution using the knife-edge scanning microscope. *BMC Neuroscience*, 11(Suppl 1):P136. Nineteenth Annual Computational Neuroscience Meeting: CNS*2010.
- [16] Choe, Y., Mayerich, D., Kwon, J., Miller, D. E., Chung, J. R., Sung, C., Keyser, J., and Abbott, L. C. (2011). Knife-edge scanning microscopy for connectomics research. In *Proceedings of the International Joint Conference on Neural Networks*, 2258–2265. Piscataway, NJ: IEEE Press.
- [17] Choe, Y., Mayerich, D., Kwon, J., Miller, D. E., Sung, C., Chung, J. R., Huffman, T., Keyser, J., and Abbott, L. C. (2011). Specimen preparation, imaging, and analysis protocols for knife-edge scanning microscopy. *Journal of Visualized Experiments*, 58:e3248. Doi: 10.3791/3248.
- [18] Choe, Y., and Miikkulainen, R. (2004). Contour integration and segmentation in a self-organizing map of spiking neurons. *Biological Cybernetics*, 90:75–88.
- [19] Choe, Y., Sung, C., Choi, J., Srivastava, M., Priour, M. R., Mayerich, D., Keyser, J., and Abbott, L. C. (2014). Open web atlas for high-resolution 3d mouse brain data. In *Neuroscience Meeting Planner, Washington, DC: Society for Neuroscience*. Program No. 185.02. Online.
- [20] Choi, H., and Choi, S. (2004). Kernel Isomap. *Electronics Letters*, 40:1612–1613.
- [21] Choi, H., and Choi, S. (2007). Robust kernel Isomap. *Pattern Recognition*, 40(3):853–862.
- [22] Choi, H., Choi, S., and Choe, Y. (2008). Manifold integration with markov random walks. In *Proceedings of the 23rd National Conference on Artificial Intelligence(AAAI 2008)*, 424–429.
- [23] Choi, J. (2013). *Knife-Edge Scanning Microscope Mouse Brain Atlas in Vector Graphics for Enhanced Performance*. Master's thesis, Department of Computer Science and Engineering, Texas A&M University.
- [24] Chung, J. R., Sung, C., Mayerich, D., Kwon, J., Miller, D. E., Huffman, T., Abbott, L. C., Keyser, J., and Choe, Y. (2011). Multiscale exploration of mouse brain microstructures using the knife-edge scanning microscope brain atlas. *Frontiers in Neuroinformatics*, 5:29.
- [25] David-Jürgens, M., Churs, L., Berkefeld, T., Zepka, R., and Dinse, H. (2008). Differential effects of aging on fore-and hindpaw maps of rat somatosensory cortex. *PLoS One*, 3(10):e3399–e3399.
- [26] DeFelipe, J. (1993). Neocortical neuronal diversity: chemical heterogeneity revealed by colocalization studies of classic neurotransmitters, neuropeptides, calcium-binding proteins, and cell surface molecules. *Cerebral Cortex*, 3(4):273–289.

- [27] Deibert, E., Kraut, M., Kremen, S., and Hart, J. (1999). Neural pathways in tactile object recognition. *Neurology*, 52:1413–1417.
- [28] Diamond, M. E., von Heimendahl, M., Knutsen, P. M., Kleinfeld, D., and Ahissar, E. (2008). ‘where’and‘what’in the whisker sensorimotor system. *Nature Reviews Neuroscience*, 9(8):601–612.
- [29] DiCarlo, J. J., and Johnson, K. O. (2000). Spatial and temporal structure of receptive fields in primate somatosensory area 3b: Effects of stimulus scanning direction and orientation. *Neuroscience*, 20:495–510.
- [30] DiCarlo, J. J., Johnson, K. O., and Hsiao, S. S. (1998). Structure of receptive fields in area 3b of primary somatosensory cortex in the alert monkey. *The Journal of neuroscience*, 18(7):2626–2645.
- [31] Dileepkumar, A. (2014). *Semi-Automated Reconstruction of Vascular Networks in Knife-Edge Scanning Microscope Mouse Brain Data*. Master’s thesis, Department of Computer Science and Engineering, Texas A&M University.
- [32] Efros, A. A., and Leung, T. K. (1999). Texture Synthesis by Non-parametric Sampling. In *IEEE International Conference on Computer Vision*, 1033–1038. Corfu, Greece.
- [33] Field, D. J. (1987). Relations between the statistics of natural images and the response properties of cortical cells. *Journal of the Optical Society of America A*, 4:2379–2394.
- [34] Foffani, G., Tutunculer, B., and Moxon, K. A. (2004). Role of spike timing in the forelimb somatosensory cortex of the rat. *The Journal of neuroscience*, 24(33):7266–7271.
- [35] Fogel, I., and Sagi, D. (1989). Gabor filters as texture discriminator. *Biological Cybernetics*, 61:102–113.
- [36] Genisman, Y., Gundersen, H., Van Der Zee, E., and West, M. (1996). Unbiased stereological estimation of the total number of synapses in a brain region. *Journal of neurocytology*, 25(1):805–819.
- [37] Guo, Z. V., Hires, S. A., Li, N., O’Connor, D. H., Komiyama, T., Ophir, E., Huber, D., Bonardi, C., Morandell, K., Gutnisky, D., et al. (????). Procedures for behavioral experiments in head-fixed mice. *PLoS One*, 9.
- [38] Han, D., Keyser, J., and Choe, Y. (2009). A local maximum intensity projection tracing of vasculature in Knife-Edge Scanning Microscope volume data. In *Proceedings of the IEEE International Symposium on Biomedical Imaging*, 1259–1262.
- [39] He, Z. J., and Nakayama, K. (1994). Perceiving textures: Beyond filtering. *Vision Research*, 34:151–62.
- [40] Heess, N., Williams, C. K. I., and Hinton, G. E. (2009). Learning generative texture models with extended fields-of-experts. In *Proceedings of the British Machine Vision Conference*. In press.
- [41] Hodgkin, A. L., and Huxley, A. F. (1952). A quantitative description of membrane current and its application to conduction and excitation in nerve. *Journal of Physiology*, 117:500–544.

- [42] Hoyer, P. O., and Hyvärinen, A. (2000). Independent component analysis applied to feature extraction from colour and stereo images. *Network: Computation in Neural Systems*, 11:191–210.
- [43] Hu, J., Biophysically accurate brain modeling and simulation using hybrid mpi/openmp parallel processing.
- [44] Jadhav, S. P., and Feldman, D. E. (2010). Texture coding in the whisker system. *Current opinion in neurobiology*, 20(3):313–318.
- [45] Jain, A. K., and Farrokhnia, F. (1991). Unsupervised texture segmentation using Gabor filters. *Pattern Recognition*, 24:1167–1186.
- [46] Johnson, K. O., and Hsiao, S. S. (1992). Neural mechanisms of tactal form and texture perception. *Annual review of neuroscience*, 15(1):227–250.
- [47] Jones, E. G. (2007). Neuroanatomy: Cajal and after cajal. *Brain research reviews*, 55(2):248–255.
- [48] Julesz, B. (1965). Texture and visual perception. *Scientific American*, 212:38–48.
- [49] Julesz, B. (1986). Texton gradients: the texton theory revisited. *Biol Cybern*, 54:245–251.
- [50] Julesz, B., and Bergen, J. (1982). Texton theory of preattentive vision and texture perception. *Journal of the Optical Society of America*, 72:1756.
- [51] Kaczmarek, K., Webster, J. G., Bach-y Rita, P., Tompkins, W. J., et al. (1991). Electrotactile and vibrotactile displays for sensory substitution systems. *Biomedical Engineering, IEEE Transactions on*, 38(1):1–16.
- [52] Kalisman, N., Silberberg, G., and Markram, H. (2003). Deriving physical connectivity from neuronal morphology. *Biological Cybernetics*, 88:210–218.
- [53] Kim, D. (2011). *Automatic Seedpoint Selection and Tracing of Microstructures in the Knife-Edge Scanning Microscope Mouse Brain Data Set*. Master’s thesis, Department of Computer Science, Texas A&M University, College Station, Texas.
- [54] Kim, U., and Ebner, F. F. (1999). Barrels and septa: separate circuits in rat barrel field cortex. *Journal of Comparative Neurology*, 408(4):489–505.
- [55] Kullback, S., and Leibler, R. A. (1951). On information and sufficiency. *The Annals of Mathematical Statistics*, 79–86.
- [56] Kwon, J., Lim, J., Lee, S., Mayerich, D., Keyser, J., Abbott, L. C., and Choe, Y. (2014). High-throughput and high-resolution 3d tissue scanner with internet connected 3d virtual microscope for large-scale automated histology. In *Neuroscience Meeting Planner, Washington, DC: Society for Neuroscience*. Program No. 185.15. Online.
- [57] Kwon, J., Mayerich, D., and Choe, Y. (2011). Automated cropping and artifact removal for knife-edge scanning microscopy. In *Proceedings of the IEEE International Symposium on Biomedical Imaging*, 1366–1369.

- [58] Kwon, J., Mayerich, D., Choe, Y., and McCormick, B. H. (2008). Lateral sectioning for knife-edge scanning microscopy. In *Proceedings of the IEEE International Symposium on Biomedical Imaging*, 1371–1374.
- [59] Lal Das, S. (2014). *Cell Detection in Knife-Edge Scanning Microscopy Images of Nissl-stained Mouse and Rat Brain Samples using Random Forests*. Master’s thesis, Department of Computer Science and Engineering, Texas A&M University.
- [60] Lal Das, S., Keyser, J., and Choe, Y. (2015). Random-forest-based automated cell detection in knife-edge scanning microscope rat nissl data. In *Proceedings of the International Joint Conference on Neural Networks*. DOI: 10.1109/IJCNN.2015.7280852.
- [61] Lee, H.-C., and Choe, Y. (2003). Detecting salient contours using orientation energy distribution. In *Proceedings of the International Joint Conference on Neural Networks*, 206–211. IEEE.
- [62] Lin, H., and Li, P. (2012). Classifying circuit performance using active-learning guided support vector machines. In *Computer-Aided Design (ICCAD), 2012 IEEE/ACM International Conference on*, 187–194.
- [63] Lin, H., and Li, P. (2014). Parallel hierarchical reachability analysis for analog verification. In *Proceedings of the 51st Annual Design Automation Conference*, DAC ’14, 150:1–150:6. New York, NY, USA: ACM.
- [64] Lin, H., and Li, P. (2015). Circuit performance classification with active learning guided sampling for support vector machines. *Computer-Aided Design of Integrated Circuits and Systems, IEEE Transactions on*, 34(9):1467 – 1480.
- [65] Lin, H., Li, P., and Myers, C. (2013). Verification of digitally-intensive analog circuits via kernel ridge regression and hybrid reachability analysis. In *Design Automation Conference (DAC), 2013 50th ACM / EDAC / IEEE*, 1–6.
- [66] Liu, X., and Wang, D. (2002). A spectral histogram model for texton modeling and texture discrimination. *Vision Research*, 42:2617–2634.
- [67] Luisi, J., Narayanaswamy, A., Galbreath, Z., and Roysam, B. (2011). The FARSIGHT trace editor: An open source tool for 3-d inspection and efficient pattern analysis aided editing of automated neuronal reconstructions. *Neuroinformatics*, 9:305–315.
- [68] Malik, J., Belongie, S., Shi, J., and Leung, T. K. (1999). Textons, contours and regions: Cue integration in image segmentation. In *ICCV(2)*, 918–925.
- [69] Malik, J., and Perona, P. (1990). Preattentive texture discrimination with early vision mechanisms. *J of Optical Soc of Am A*, 7:923–931.
- [70] Manjunath, B. S., and Chellappa, R. (1991). Unsupervised texture segmentation using markov random field models. *IEEE Trans. on Pattern Analysis and Machine Intelligence*, 13:478–482.
- [71] Maricich, S. M., Morrison, K. M., Mathes, E. L., and Brewer, B. M. (2012). Rodents rely on merkel cells for texture discrimination tasks. *The Journal of Neuroscience*, 32(10):3296–3300.

- [72] Markram, H., Muller, E., Ramaswamy, S., Reimann, M. W., Abdellah, M., Sanchez, C. A., Ailamaki, A., Alonso-Nanclares, L., Antille, N., Arsever, S., et al. (2015). Reconstruction and simulation of neocortical microcircuitry. *Cell*, 163(2):456–492.
- [73] Mayerich, D., Kwon, J., Choe, Y., Abbott, L., and Keyser, J. (2008). Constructing high-resolution microvascular models. In *Proceedings of the 3rd International Workshop on Microscopic Image Analysis with Applications in Biology (MIAAB 2008)*. Online.
- [74] Mayerich, D., Kwon, J., Panchal, A., Keyser, J., and Choe, Y. (2011). Fast cell detection in high-throughput imagery using gpu-accelerated machine learning. In *Proceedings of the IEEE International Symposium on Biomedical Imaging*, 719–723.
- [75] Mayerich, D., Kwon, J., Sung, C., Abbott, L. C., Keyser, J., and Choe, Y. (2011). Fast macro-scale transmission imaging of microvascular networks using KESM. *Biomedical Optics Express*, 2:2888–2896.
- [76] Mayerich, D., McCormick, B. H., and Keyser, J. (2007). Noise and artifact removal in knife-edge scanning microscopy. In *Proceedings of the IEEE International Symposium on Biomedical Imaging*, 556–559.
- [77] McCormick, B. H. (2003). The knife-edge scanning microscope. Technical report, Department of Computer Science, Texas A&M University. <http://research.cs.tamu.edu/bnl/>.
- [78] McCormick, B. H., System and method for imaging an object. USPTO patent #US 6,744,572 (for Knife-Edge Scanning; 13 claims).
- [79] McCormick, B. H., and Mayerich, D. M. (2004). Three-dimensional imaging using Knife-Edge Scanning Microscope. *Microscopy and Microanalysis*, 10 (Suppl. 2):1466–1467.
- [80] McDermott, J. H., and Simoncelli, E. P. (2011). Sound texture perception via statistics of the auditory periphery: evidence from sound synthesis. *Neuron*, 71(5):926–940.
- [81] Mehta, S. B., and Kleinfeld, D. (2004). Frisking the whiskers: patterned sensory input in the rat vibrissa system. *Neuron*, 41(2):181–184.
- [82] Miikkulainen, R., Bednar, J. A., Choe, Y., and Sirosh, J. (2005). *Computational Maps in the Visual Cortex*. Berlin: Springer. URL: <http://www.computationalmaps.org>. 538 pages.
- [83] Mika, S., Ratsch, G., Weston, J., Schölkopf, B., and Müller, K. (1999). Fisher discriminant analysis with kernels. In *Proceedings of IEEE Neural Networks for Signal Processing Workshop*, 41–48.
- [84] Miller, D. E. (2014). *A Combined Skeleton Model*. Master's thesis, Department of Computer Science and Engineering, Texas A&M University.
- [85] Mukherjee, P., Amin, C. S., and Li, P. (2014). Approximate property checking of mixed-signal circuits. In *Proceedings of the 51st Annual Design Automation Conference*, DAC '14, 115:1–115:6. New York, NY, USA: ACM.
- [86] Mukherjee, P., and Li, P. (2014). Leveraging pre-silicon data to diagnose out-of-specification failures in mixed-signal circuits. In *Proceedings of the 51st Annual Design Automation Conference*, DAC '14, 9:1–9:6. New York, NY, USA: ACM.

- [87] Nakayama, K., He, Z. J., and Shimojo, S. (1995). Visual surface representation: A critical link between lower-level and higher-level vision. In Kosslyn, S. M., and Osherson, D. N., editors, *An Invitation to Cognitive Science: Vol. 2 Visual Cognition*, 1–70. Cambridge, MA: MIT Press. Second edition.
- [88] Niell, C. M., and Stryker, M. P. (2008). Highly selective receptive fields in mouse visual cortex. *The Journal of neuroscience*, 28(30):7520–7536.
- [89] Oh, S., and Choe, Y. (2007). Segmentation of textures defined on flat vs. layered surfaces using neural networks: Comparision of 2d vs. 3d representations. *Neurocomputing*, 70:2245–2255.
- [90] O’Leary, D. D. (1989). Do cortical areas emerge from a protocortex? *Trends in neurosciences*, 12(10):400–406.
- [91] Olshausen, B. A., and Field, D. J. (1996). Emergence of simple-cell receptive field properties by learning a sparse code for natural images. *Nature*, 381:607–609.
- [92] Paragios, N., and Deriche, R. (2002). Geodesic active regions and level set methods for supervised texture segmentation. *International Journal of Computer Vision*, 46:223–247.
- [93] Park, C. (2009). *Performance, Development, and Analysis of Tactile vs. Visual Receptive Fields in Texture Tasks*. PhD thesis, Department of Computer Science, Texas A&M University.
- [94] Park, C., Bai, Y. H., and Choe, Y. (2009). Tactile or visual?: Stimulus characteristics determine receptive field type in a self-organizing map model of cortical development. In *Proceedings of the 2009 IEEE Symposium on Computational Intelligence for Multimedia Signal and Vision Processing*, 6–13. **Best Student Paper Award**.
- [95] Park, C., Choi, H., and Choe, Y. (2009). Self-organization of tactile receptive fields: Exploring their textural origin and their representational properties. In *Advances in Self-Organizing Maps: Proceedings of the 7th International Workshop, WSOM 2009. LNCS 5629*, 228–236. Heidelberg: Springer.
- [96] Peng, H., Bria, A., Zhou, Z., Iannello, G., and Long, F. (2014). Extensible visualization and analysis for multidimensional images using Vaa3D. *Nature protocols*, 9(1):193–208.
- [97] Picard, D., Dacremont, C., Valentin, D., and Giboreau, A. (2003). Perceptual dimensions of tactile textures. *Acta psychologica*, 114(2):165–184.
- [98] Portilla, J., and Simoncelli, E. P. (2000). A parametric texture model based on joint statistics of complex wavelet coefficients. *International Journal of Computer Vision*, 40:49–71.
- [99] Reinagel, P., and Laughlin, S. (2001). Editorial: Natural stimulus statistics. *Network: Computation in Neural Systems*, 12:237–240.
- [100] Reinagel, P., and Zador, A. M. (1999). Natural scene statistics at the center of gaze. *Network: Computation in Neural Systems*, 10:341–350.
- [101] Reiner, A., Veenman, C. L., Medina, L., Jiao, Y., Del Mar, N., and Honig, M. G. (2000). Pathway tracing using biotinylated dextran amines. *Journal of neuroscience methods*, 103(1):23–37.

- [102] Sarma, S., and Choe, Y. (2006). Salience in orientation-filter response measured as suspicious coincidence in natural images. In Gil, Y., and Mooney, R., editors, *Proceedings of the 21st National Conference on Artificial Intelligence (AAAI 2006)*, 193–198.
- [103] Schölkopf, B., and Smola, A. J. (2002). *Learning with Kernels*. MIT Press.
- [104] Sejnowski, T. J. (1986). Open questions about computation in cerebral cortex. *Parallel distributed processing*, 2:372–389.
- [105] Sharma, J., Angelucci, A., and Sur, M. (2000). Induction of visual orientation modules in auditory cortex. *Nature*, 404:841–847.
- [106] Shepherd, G. M., Pologruto, T. A., and Svoboda, K. (2003). Circuit analysis of experience-dependent plasticity in the developing rat barrel cortex. *Neuron*, 38(2):277–289.
- [107] Shepherd, G. M., Stepanyants, A., Bureau, I., Chklovskii, D., and Svoboda, K. (2005). Geometric and functional organization of cortical circuits. *Nature neuroscience*, 8(6):782–790.
- [108] Singhal, A. (2015). *Skeletonization-Based Automated Tracing and Reconstruction of Neuronal Networks in Knife-Edge Scanning Microscope Mouse Brain India Ink Data*. Master's thesis, Department of Computer Science and Engineering, Texas A&M University.
- [109] Srivastava, M. (2015). *Knife-Edge Scanning Microscope Brain Atlas Interface for Tracing and Analysis of Vasculature Data*. Master's thesis, Department of Computer Science and Engineering, Texas A&M University.
- [110] Sung, C. (2013). *Exploration, Registration, and Analysis of High-Throughput 3D Microscopy Data from the Knife-Edge Scanning Microscope*. PhD thesis, Department of Computer Science and Engineering, Texas A&M University.
- [111] Sung, C., Chung, J. R., Mayerich, D., Kwon, J., Miller, D. E., Huffman, T., Keyser, J., Abbott, L. C., and Choe, Y. (2011). Knife-edge scanning microscope brain atlas: A submicrometer-resolution web-based mouse brain atlas. In *Neuroscience Meeting Planner, Washington, DC: Society for Neuroscience*. Program No. 328.05. Online.
- [112] Sung, C., Mayerich, D., Kwon, J., Miller, D. E., Abbott, L. C., Keyser, J., Huffman, T., and Choe, Y. (2012). Web-based knife-edge scanning microscope brain atlas in vector-graphics for enhanced performance. In *Neuroscience Meeting Planner, New Orleans, LA: Society for Neuroscience*. Program No. 328.05. Online.
- [113] Sung, C., Woo, J., Goodman, M., Huffman, T., and Choe, Y. (2013). Scalable, incremental learning with MapReduce parallelization for cell detection in high-resolution 3D microscopy data. In *Proceedings of the International Joint Conference on Neural Networks*, 434–440.
- [114] Teeters, J. L., Harris, K. D., Millman, K. J., Olshausen, B. A., and Sommer, F. T. (2008). Data sharing for computational neuroscience. *Neuroinformatics*, 6(1):47–55.
- [115] Tenenbaum, J. B., de Silva, V., and Langford, J. C. (2000). A global geometric framework for nonlinear dimensionality reduction. *Science*, 290:2319–2323.
- [116] Thielscher, A., Kölle, M., Neumann, H., Spitzer, M., and Grön, G. (2008). Texture segmentation in human perception: A combined modeling and fmri study. *Neuroscience*, 151(3):730–736.

- [117] Thielscher, A., and Neuman, H. (2006). A computational model to link psychophysics and cortical cell activation patterns in human texture processing. *J of Comp Neurosci*, 22:255–282.
- [118] Varma, M., and Zisserman, A. (2003). Texture classification: Are filter banks necessary? In *Proceedings of 2003 IEEE Computer Society Conference on Computer Vision and Pattern Recognition (CVPR 2003)*, 691–698.
- [119] Varma, M., and Zisserman, A. (2005). A statistical approach to texture classification from single images. *International Journal of Computer Vision*, 62:61–81.
- [120] Von Heimendahl, M., Itskov, P. M., Arabzadeh, E., and Diamond, M. E. (2007). Neuronal activity in rat barrel cortex underlying texture discrimination. *PLoS Biol*, 5(11):e305.
- [121] Wang, M., Yan, B., Hu, J., and Li, P. (2011). Simulation of large neuronal networks with biophysically accurate models on graphics processors. In *Neural Networks (IJCNN), The 2011 International Joint Conference on*, 3184–3193. IEEE.
- [122] Wei, L.-Y., and Levoy, M. (2000). Fast texture synthesis using tree-structured vector quantization. In *SIGGRAPH '00: Proceedings of the 27th Annual Conference on Computer Graphics and Interactive Techniques*, 479–488.
- [123] Wetzel, C., Hu, J., Riethmacher, D., Benckendorff, A., Harder, L., Eilers, A., Moshourab, R., Kozlenkov, A., Labuz, D., Caspani, O., et al. (2007). A stomatin-domain protein essential for touch sensation in the mouse. *Nature*, 445(7124):206–209.
- [124] Williams, R. W., and Rakic, P. (1988). Three-dimensional counting: An accurate and direct method to estimate numbers of cells in sectioned material. *Journal of Comparative Neurology*, 278(3):344–352.
- [125] Wolfe, J., Hill, D. N., Pahlavan, S., Drew, P. J., Kleinfeld, D., and Feldman, D. E. (2008). Texture coding in the rat whisker system: slip-stick versus differential resonance. *PLoS Biol*, 6(8):e215.
- [126] Wong, A., and Brown, R. (2006). Visual detection, pattern discrimination and visual acuity in 14 strains of mice. *Genes, Brain and Behavior*, 5(5):389–403.
- [127] Yan, B., and Li, P. (2011). An integrative view of mechanisms underlying generalized spike-and-wave epileptic seizures and its implication on optimal therapeutic treatments. *PLoS One*, 6:e22440.
- [128] Yan, B., and Li, P. (2011). Reduced order modeling of passive and quasi-active dendrites for nervous system simulation. *Journal of computational neuroscience*, 31(2):247–271.
- [129] Yan, B., and Li, P. (2013). The emergence of abnormal hypersynchronization in the anatomical structural network of human brain. *NeuroImage*, 65:34–51.
- [130] Yang, H.-F., and Choe, Y. (2009). Cell tracking and segmentation in electron microscopy images using graph cuts. In *Proceedings of the IEEE International Symposium on Biomedical Imaging*, 306–309.
- [131] Yang, H.-F., and Choe, Y. (2010). Electron microscopy image segmentation with estimated symmetric three-dimensional shape prior. In *Proceedings of the 6th International Symposium on Visual Computing*.

- [132] Yang, H.-F., and Choe, Y. (2011). An interactive editing framework for electron microscopy image segmentation. In *Proceedings of the 7th International Symposium on Visual Computing (LNCS 6938)*, 400–409.
- [133] Yang, W. (2014). *Automated neurovascular tracing and analysis of the Knife-Edge Scanning Microscope India ink data set*. Master’s thesis, Department of Computer Science and Engineering, Texas A&M University.
- [134] Yin, L., Deng, Y., and Li, P. (2012). Verifying dynamic properties of nonlinear mixed-signal circuits via efficient smt-based techniques. In *Computer-Aided Design (ICCAD), 2012 IEEE/ACM International Conference on*, 436–442.
- [135] Yin, L., Deng, Y., and Li, P. (2013). Simulation-assisted formal verification of nonlinear mixed-signal circuits with bayesian inference guidance. *Computer-Aided Design of Integrated Circuits and Systems, IEEE Transactions on*, 32(7):977–990.
- [136] Yoshioka, T., Gibb, B., Dorsch, A. K., Hsiao, S. S., and Johnson, K. O. (2001). Neural coding mechanisms underlying perceived roughness of finely textured surfaces. *The Journal of Neuroscience*, 21(17):6905–6916.
- [137] Zhang, J., Tan, T., and Ma, L. (2002). Invariant texture segmentation via circular Gabor filters. *16 th International Conference on Pattern Recognition (ICPR’02)*, 2.
- [138] Zhang, W. (2014). *Real-time Image Error Detection in Knife-Edge Scanning Microscope*. Master’s thesis, Department of Computer Science and Engineering, Texas A&M University.
- [139] Zhang, W., Yoo, J., Keyser, J., Abbott, L. C., and Choe, Y. (2015). Real-time detection of imaging errors in the knife-edge scanning microscope through change detection. In *Proceedings of the IEEE International Symposium on Biomedical Imaging*. Accepted.
- [140] Zhang, Y., Li, P., Jin, Y., and Choe, Y. (2015). A digital liquid state machine with biologically inspired learning and its application to speech recognition. *IEEE Transactions on Neural Networks and Learning Systems*. In press.
- [141] Zhang, Y., Yan, B., Wang, M., Hu, J., Lu, H., and Li, P. (2012). Linking brain behavior to underlying cellular mechanisms via large-scale brain modeling and simulation. *Neurocomputing*, 97:317–331.
- [142] Zhu, L., Chen, Y., Freeman, B., and Torralba, A. (2009). Nonparametric bayesian texture learning and synthesis. In Bengio, Y., Schuurmans, D., Lafferty, J., Williams, C. K. I., and Culotta, A., editors, *Advances in Neural Information Processing Systems 22 (NIPS 2009)*, 2313–2321.
- [143] Zhu, S. C., Wu, Y., and Mumford, D. (1998). Filters, Random Fields and Maximum Entropy (FRAME): Towards a unified theory for texture modeling. *Int. J. Comput. Vision*, 27(2):107–126.